Macromolecules

Article

Cite This: Macromolecules 2019, 52, 3049−3055

pubs.acs.org/Macromolecules

Insights into the Kinetics of Supramolecular Comonomer Incorporation in Water

René P. M. Lafleur,[†] Sandra M. C. Schoenmakers,[†] Pranav Madhikar,[†,‡] Davide Bochicchio,[§] Björn Baumeier,[†,‡] Anja R. A. Palmans,[†] Giovanni M. Pavan,[§] and E. W. Meijer*[,†]

[†]Institute for Complex Molecular Systems and [‡]Department of Mathematics and Computer Science, Eindhoven University of Technology, P.O. Box 513, 5600 MB Eindhoven, The Netherlands

[§]Department of Innovative Technologies, University of Applied Sciences and Arts of Southern Switzerland, Galleria 2, Via Cantonale 2c, CH-6928 Manno, Switzerland

Supporting Information

ABSTRACT: Multicomponent supramolecular polymers are a versatile platform to prepare functional architectures, but a few studies have been devoted to investigate their noncovalent synthesis. Here, we study supramolecular copolymerizations by examining the mechanism and time scales associated with the incorporation of new monomers in benzene-1,3,5-tricarboxamide (BTA)-based supramolecular polymers. The BTA molecules in this study all contain three tetra(ethylene glycol) chains at the periphery for water solubility but differ in their alkyl chains that feature either 10, 12 or 13 methylene units. C_{10}BTA does not form ordered supramolecular assemblies, whereas C_{12}BTA and C_{13}BTA both form high aspect ratio supramolecular polymers. First, we illustrate that C_{10}BTA can mix into the supramolecular polymers based on either C_{12}BTA or C_{13}BTA by comparing the temperature response of the equilibrated mixtures to the temperature response of the individual components in water. Subsequently, we mix C_{10}BTA with the polymers and follow the copolymerization over time with UV spectroscopy and hydrogen/deuterium exchange mass spectrometry experiments. Interestingly, the time scales obtained in both experiments reveal significant differences in the rates of copolymerization. Coarse-grained simulations are used to study the incorporation pathway and kinetics of the C_{10}BTA monomers into the different polymers. The results demonstrate that the kinetic stability of the host supramolecular polymer controls the rate at which new monomers can enter the existing supramolecular polymers.

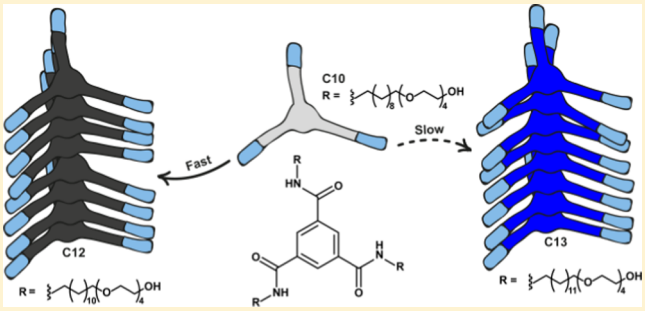

INTRODUCTION

Supramolecular polymers are ideal candidates for the development of functional architectures because their dynamic nature provides access to a versatile set of copolymers by the mixing of different building blocks. The combination of different monomers can result in multicomponent supramolecular polymers with properties that are difficult to attain with single-component systems. For example, supramolecular copolymers in water have already been successfully prepared for the introduction of bioactivity,[1−5] to enable drug delivery,[6,7] and for imaging.[8,9] Moreover, this modular approach has also been used to acquire a fundamental understanding of the dynamics of aqueous supramolecular polymers.[1,10−13] Since the majority of these polymers are able to form hydrogels, supramolecular multicomponent materials with unique thermal,[14] electronic,[15] and mechanical properties are emerging.[16,17]

Essential for the further development of supramolecular copolymers in water is an increased understanding of the features that govern their assembly kinetics.[18] This requires a combination of time-resolved measurements and systematic changes of the building blocks. Although small changes in the molecular structure are already expanding the control over assembly pathways in organic solvents,[19−21] the translation to an aqueous environment is notoriously challenging. First, when changing the hydrophobic/hydrophilic balance, the compounds may become either too soluble (no aggregation) or too insoluble and precipitate. Second, small changes in the molecular structure often lead to large morphological changes of the supramolecular aggregates.[22−24] These subtleties are also reflected in the assembly of supramolecular copolymers in water because often this requires thoughtful solution processing methodologies.[25−27] Most probably, due to these challenges, the principles that determine the kinetics of supramolecular copolymerization in water are so far elusive.

Currently, only a few laboratories have studied the kinetics of supramolecular copolymerization of small molecules in water.[25,27,28] For example, the Würthner group has examined

Received: February 11, 2019
Revised: March 21, 2019
Published: April 9, 2019

DOI: 10.1021/acs.macromol.9b00300
Macromolecules 2019, 52, 3049−3055

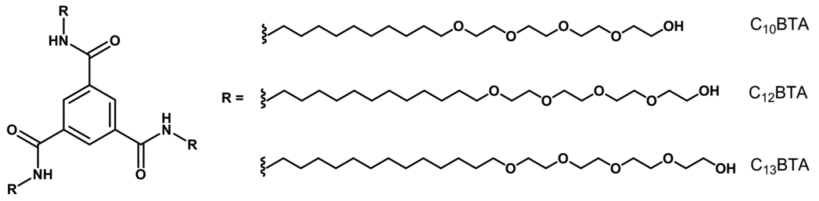

Figure 1. Chemical structures of C_{10}BTA, C_{12}BTA, and C_{13}BTA.

the copolymerization of two amphiphilic perylene diimide dyes into an $(A_mBB)_n$ structure using ^{1}H NMR spectroscopy.[25] The copolymerization was initiated by adding water to the dissolved monomers in tetrahydrofuran. Besenius and co-workers investigated the kinetics of copolymerization into $(AB)_n$-type polymers using dendritic anionic and cationic peptide monomers.[28] The monomers assembled based on electrostatic interactions, and the resulting structures have additionally been investigated using molecular dynamics (MD) simulations.[29] Recent developments in kinetic models and coarse-grained (CG) molecular simulations now enable theoretical studies on the time development of supramolecular copolymers.[30,31] For example, high-resolution (<5 Å) CG simulations allowed us to observe that monomers can diffuse along the surface of supramolecular polymers without detaching from the polymer.[32,33]

Our group has recently prepared supramolecular copolymers based on amphiphilic benzene-1,3,5-tricarboxamide (BTA) derivatives.[34] We first discovered that small changes in the length of the alkyl chains, that form the hydrophobic pocket, can be used to tune the stability of homopolymers.[35,36] Subsequently, we mixed two different monomers that both have alkyl chains composed of 12 methylene units but differ in their water-solubilizing groups by having either dendronized or linear ethylene glycol chains at their peripheries.[34] Several copolymers were prepared by shortly heating two-component mixtures that have the monomers present in different ratios. It was shown that the ratio of the monomers could be used to tune the dynamic behavior of the equilibrated supramolecular copolymers.

Here, we present our study on the time scales and mechanism involved in the spontaneous and dynamic formation of supramolecular copolymers using three water-soluble BTA derivatives (Figure 1). To this end, a monomer that is not able to form supramolecular polymers by itself (C_{10}BTA) is added to polymers formed from either C_{12}BTA or C_{13}BTA. Both experiments and simulations lead to the conclusion that the stability of the host polymer determines the rate at which new monomers are incorporated in the supramolecular polymers.

RESULTS AND DISCUSSION

As a reference, we first prepared single-component supramolecular aggregates from the monomers displayed in Figure 1 using a heating–cooling protocol (see Supporting Information). Turbidity measurements were then performed by monitoring the optical density (O.D.) as a function of temperature. The O.D. was measured at a wavelength at which the BTAs do not absorb UV light (340 nm). We observed a sharp decrease in the O.D. upon cooling, which is a result of the lower critical solution temperature (LCST) of the tetra(ethylene glycol) side chains.[37] The cloud point temperature (T_{cp}) shifts to a higher temperature when the length of the alkyl chains increases (Figure 2, gray lines). Curiously, for the polymers formed from C_{12}BTA and C_{13}BTA, a second

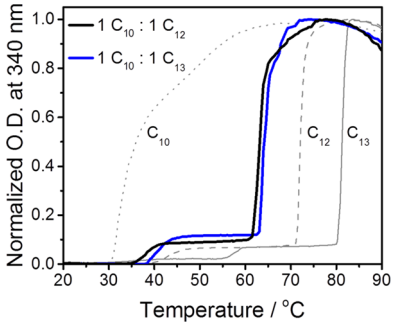

Figure 2. Normalized optical density at 340 nm as a function of temperature for the single-component aggregates, C_{10}BTA (gray, dot, T_{cp} = 30 °C), C_{12}BTA (gray, dash, T_{cp} = 71 °C), and C_{13}BTA (gray, solid, T_{cp} = 80 °C), and the copolymers of C_{10}BTA and C_{12}BTA (black) and C_{10}BTA and C_{13}BTA (blue). The cooling rate was 0.2 °C/min, the concentration was 50 μM, the path length of the quartz cuvette used was 1 cm, and the measurements were performed without stirring.

transition was observed that occurred at lower temperatures. This transition was previously also observed in micellar assemblies and defined as the sub-LCST.[38] A possible explanation for this phenomenon is conformational rigidity of the molecules that could be induced by hydrogen bonds.[39] Indeed, with infrared spectroscopy performed at room temperature, we observed that the polymers formed from C_{12}BTA and C_{13}BTA are stabilized by hydrogen bonds, whereas the aggregates formed from C_{10}BTA are not (see Supporting Information Figure S1).

To form dual-component aggregates containing C_{10}BTA and any one of the other BTAs, we simply combined equimolar solutions of the individual aggregates and stored them for 24 h at room temperature. Subsequently, the same turbidity measurements were performed (Figure 2, colored lines) and we compare the T_{cp} of the copolymers with those of the single-component aggregates. The T_{cp}'s of the mixtures shifted to 61.5 °C (C_{10}BTA–C_{12}BTA) and 63 °C (C_{10}BTA–C_{13}BTA), which are both in between the T_{cp}'s of the constituent monomers. Although the cooling curves show the clearest transitions, also the corresponding heating curves display intermediate T_{cp}'s (see Supporting Information Figure S2). These results indicate that (1) supramolecular copolymers can be prepared simply by mixing of the solutions and waiting and (2) that the C_{10}BTAs are most likely randomly incorporated in the supramolecular copolymers. Cryogenic transmission electron microscopy (Cryo-TEM) experiments show the existence of one-dimensional supramolecular polymers with a high aspect ratio, indicating that the morphology did not change after mixing (see Supporting Information Figure S3).

DOI: 10.1021/acs.macromol.9b00300
Macromolecules 2019, 52, 3049–3055

The kinetics of the copolymerization, i.e., the rate at which C_{10}BTA will be incorporated in the polymers formed from C_{12}BTA and C_{13}BTA upon mixing, was studied next. The C_{10}BTA absorbs UV light with a single absorption maximum at 207 nm, whereas the other BTAs have absorption maxima at around 211 and 226 nm.[35] The UV spectra of the equilibrated mixtures resemble the UV spectra of the host polymers, rather than displaying a superposition of the two components (see Supporting Information Figure S4). Hence, the C_{10}BTA molecules that become incorporated in the polymers adopt a molecular arrangement that is similar to that of the molecules of the host polymer. We use the large difference between the UV absorption of the C_{10}BTA and the equilibrated copolymers to monitor the kinetics of the copolymerization. The measurements were performed at a wavelength of 229 nm, and the BTAs were mixed at a 1:1 molar ratio with a stopped-flow setup. We observed that the UV absorption of the mixtures increases over time when C_{10}BTA monomers enter the polymers (Figure 3). Within 15 min, the UV absorption of

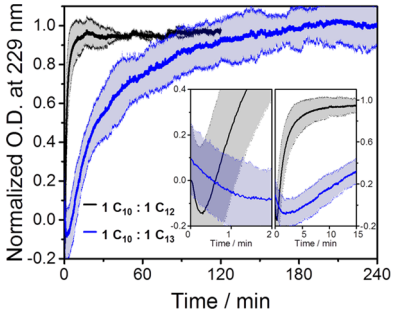

Figure 3. Normalized UV absorption at 229 nm as a function of the copolymerization time of C_{10}BTA with C_{12}BTA (black) and C_{13}BTA (blue). The insets show a zoom of the first 2 min (left) and the first 15 min (right). The lines are an average of three measurements and the surrounding areas represent one standard deviation of uncertainty. All measurements were performed at a concentration of 50 μM, at 20 °C, and using a 1 cm path length cuvette.

the copolymers of C_{10}BTA and C_{12}BTA reaches a plateau (Figure 3, right inset), indicating that C_{10}BTA is rapidly accommodated within the molecular packing of the host polymer. In sharp contrast, the copolymers of C_{10}BTA and C_{13}BTA take 4 h to equilibrate. To allow a quantitative comparison of the copolymerization kinetics, we fitted the kinetic UV absorption data with monoexponential growth functions, starting from the minima in the UV absorbance (see Supporting Information). The time to reach 50% of the UV absorbance value that corresponds to the equilibrium situation (t_{50}) was calculated to be 1.4 ± 0.6 min for C_{10}BTA and C_{12}BTA and 29.2 ± 10.7 min for C_{10}BTA and C_{13}BTA. Previously, polymers formed from C_{13}BTA were observed to exhibit slower monomer exchange dynamics as compared to those formed from C_{12}BTA,[36] indicating that a higher stability of the host polymer retards the formation of a dual-component polymer.

The use of the stopped-flow setup allowed us to detect also interesting kinetic phenomena that occurred within the first minutes after mixing. Peculiarly, during the initial seconds (C_{12}BTA) and minutes (C_{13}BTA), the UV absorption of the mixtures decreased (Figure 3, left inset). Since these effects were not observed when mixing BTA solutions of the same kind (see Supporting Information Figure S5), they are not caused by the mixing process but they may be a consequence of C_{10}BTA monomers that initially interfere with the molecular arrangement of the single-component polymers. However, no detailed interpretation is available at this time.

To further examine the time development of the copolymerizations, we developed a methodology that is inspired by the well-established biochemical "pulse-labeling" hydrogen/deuterium exchange (HDX) technique.[40] We started the copolymerizations by mixing C_{10}BTA with one of the polymers. The solutions of the single components in H_2O were mixed at room temperature and at a 1:1 molar ratio. After mixing, samples were taken at multiple time points and diluted into D_2O to allow hydrogen/deuterium exchange. These samples were analyzed by electrospray ionization mass spectrometry (MS) 90 s after the dilution into D_2O, to evaluate the extent of deuteration of C_{10}BTA. For a detailed description of this methodology, we refer to the Supporting Information.

In the solutions that contain only C_{10}BTA, we observed that the dilution of C_{10}BTA in D_2O immediately causes full deuteration of both the alcohols and the amides (C_{10}BTA-6D).[36] However, in mixtures with C_{12}BTA or C_{13}BTA, also C_{10}BTA-3D can be observed (see Supporting Information Figure S6). The alcohols at the periphery of the monomers are always in contact with water; hence, C_{10}BTA-3D contains three deuterated alcohols and the amides have not been exchanged. This indicates that when a C_{10}BTA monomer enters a polymer the amides become buried in the hydrophobic environment of the polymers and may be engaged in hydrogen bonding with other monomers.

We plotted the percentage of C_{10}BTA-3D as a function of the mixing time (Figure 4) and observed that the percentage of

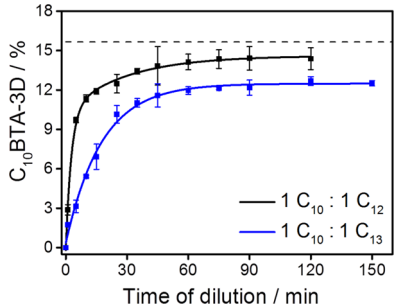

Figure 4. Percentage of C_{10}BTA-3D as a function of the mixing time (the time points at which aliquots were diluted into D_2O), when mixed at t = 0 min with polymers formed from C_{12}BTA (black) and C_{13}BTA (blue). The data points are the average of three separate measurements and the error bars represent one standard deviation of uncertainty. The solid lines are the fitted exponential growth functions. The dashed line is the average percentage of C_{10}BTA-3D obtained after 26 h of copolymerization with C_{12}BTA. All experiments were performed at room temperature (~20 °C) and at a concentration of 50 μM.

C_{10}BTA-3D in polymers formed from C_{12}BTA increases faster as compared to those formed from C_{13}BTA. The concomitant decrease in the percentage of C_{10}BTA-6D shows a similar trend and decreases faster in the presence of C_{12}BTA as compared to C_{13}BTA (see Supporting Information Figure S7). This indicates that the incorporation of C_{10}BTA in polymers formed from C_{12}BTA occurs more rapidly as compared to those formed from C_{13}BTA. To compare the time scales of the different copolymerizations quantitatively, we fitted the data

DOI: 10.1021/acs.macromol.9b00300
Macromolecules 2019, 52, 3049−3055

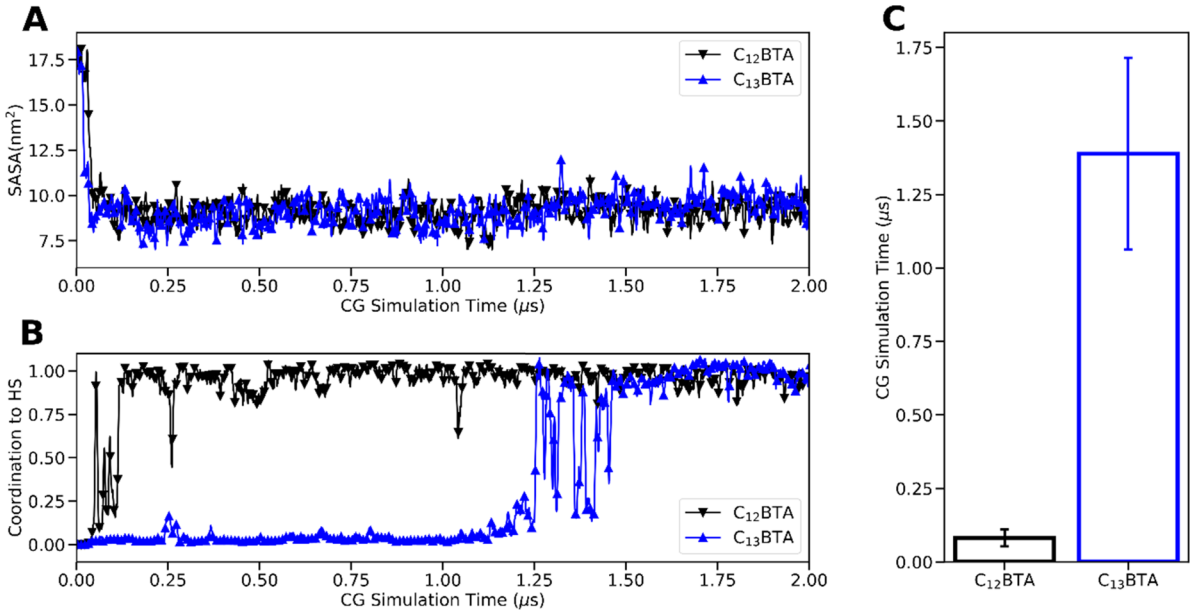

Figure 5. Mean time-to-hotspot for a C_{10}BTA monomer on C_{12}BTA and C_{13}BTA polymers obtained by CG-MD simulations. (A, B) Data from one representative CG-MD run: (A) solvent accessible surface area (SASA) and (B) coordination to hotspot of the C_{10}BTA monomer during the process of adsorption−diffusion−incorporation in a C_{12}BTA (black) and a C_{13}BTA polymer (blue). (C) Average times to coordinate with a hotspot, calculated using 10 CG-MD runs with the error bars indicating the standard error of the mean.

with exponential growth functions. Using a statistical *F*-test, we found that the copolymerization with C_{13}BTA can be described with a single exponent, whereas the copolymerization with C_{12}BTA required two exponentials (see Supporting Information). This difference is due to the faster copolymerization with C_{12}BTA in the first minutes. From the fitting results, we calculated the time required to reach 50% of the maximum percentage of C_{10}BTA-3D (t_{50}) and found 2.9 ± 0.2 min for the mixtures with C_{12}BTA and 12.7 ± 0.7 min for the copolymerization with C_{13}BTA. Hence, also in these HDX measurements, the copolymerization of C_{10}BTA with C_{13}BTA is significantly slower as compared to the copolymerization with C_{12}BTA. The difference in the time scales is, however, smaller with HDX-MS as compared to that with the UV measurements. One explanation could be that the internal order of the copolymers that is probed with UV absorption is more sensitive to the formation of hydrogen bonds within the copolymers. Whereas the UV measurements assess the incorporation of monomers in the stack (i.e., the incorporation in the hydrogen-bonding network), the HDX-MS experiments measure the accessibility of the solvent to the amides of the monomers. These measurements are thus more generally related to the penetration of a monomer into the hydrophobic pocket of the host polymer. Nonetheless, even accounting for the differences in the two types of experiments, the results can be interpreted similarly; the incorporation of C_{10}BTA in a polymer of C_{12}BTA is faster than in a polymer of C_{13}BTA.

The dashed line in Figure 4 is the maximum percentage of C_{10}BTA-3D protected from immediate full deuteration by C_{12}BTA, which was measured after 26 h of copolymerization. The number of C_{10}BTA molecules incorporated in the polymers plateaus after a certain mixing time, indicating that there are physical limits for the incorporation of (slightly different) guest monomers into the host supramolecular polymers. Similar as during the UV absorption experiments, we have observed a reciprocal influence of the incorporation of C_{10}BTA on the dynamic behavior of the other monomers. Especially during the first minutes, the HDX behavior of C_{12}BTA and C_{13}BTA was altered (see Supporting Information Figure S8). Consistent with recent results,[34] also the equilibrated copolymers show an altered dynamic behavior as compared to the single-component polymers (see Supporting Information Figure S9).

Molecular models were built to rationalize the effects observed in the experiments and to investigate the mechanism of copolymerization at the level of single monomers. A single C_{10}BTA monomer was added to the simulation box containing either a supramolecular polymer formed from C_{12}BTA or C_{13}BTA (see Supporting Information for details). Consistent with previous observations,[32] the mechanism of incorporation of the C_{10}BTA monomer in the polymers occurs in three steps: (i) C_{10}BTA monomer adsorption on the polymer, (ii) monomer diffusion on the polymer surface, and (iii) incorporation in the stack of cores (see Supporting Information Figure S10). The latter phase occurs every time the C_{10}BTA monomer finds a hotspot, i.e., a discontinuity point along the core stack where the diffusing monomer can engage with other monomers via core−core stacking and hydrogen bonding.

We ran 10 simulations for both C_{12}BTA and C_{13}BTA to obtain meaningful statistical results. Figure 5A,B reports the results for one representative CG-MD run. The solvent accessible surface area (SASA) of the C_{10}BTA monomer (Figure 5A) is maximal in the beginning when the monomer is free in solution. Within a few nanoseconds, the SASA quickly drops when the monomer adsorbs on the polymer surface (step (i)). The initial adsorption of a C_{10}BTA monomer on both polymers is of little interest herein because this is due to how fast a C_{10}BTA monomer diffuses in the medium; in this comparison, the C_{10}BTA adsorbing monomer and the solvent (water) are the same (Figure 5A: the initial drop in SASA is the same in both systems). The SASA remains approximately constant during the remaining 2 μs simulation time (steps (ii) + (iii)). Even in step (iii), the SASA does not change; when

DOI: 10.1021/acs.macromol.9b00300
Macromolecules 2019, 52, 3049−3055

the diffusing C_{10}BTA monomer reaches a hotspot, it simply stops moving on the polymer surface and becomes involved in hydrogen bonding (see Supporting Information Figure S11). In contrast, in step (iii), the core−core coordination of the C_{10}BTA monomer changes upon stacking onto a hotspot. This value is zero when the monomer is still diffusing on the surface and increases to one when the monomer stacks onto a hotspot and engages in hydrogen bonding (Figure 5B). The coordination increases quickly when a C_{10}BTA monomer is added to a polymer formed from C_{12}BTA. On average, within 200 ns of CG-MD, the monomer adsorbs on the polymer and stacks onto a hotspot (Figure 5B, black line). Interestingly, the C_{10}BTA monomer that is adsorbed on the polymer formed from C_{13}BTA diffused on the surface of the polymer for over 1.2 μs of CG-MD, before reaching and stacking onto a hotspot (Figure 5B, blue line).

Although the estimated time scales are obtained from a simplified CG model and cannot be directly compared with the experimental ones, these are very useful to compare between the two systems. The characteristic times to the hotspot, during which the C_{10}BTA monomer diffuses along the polymers, were calculated and were significantly different from one another (Figure 5C). We found that the C_{10}BTA diffusion and incorporation takes on average 1−1.5 orders of magnitude longer in C_{13}BTA as compared to C_{12}BTA. It is important to note that based on our computational setup the time necessary to complete the process is not much influenced by the initial position of the C_{10}BTA monomer when it adsorbs on the polymer surface from the solution. The dissimilarity is mainly due to the different diffusivity of the C_{10}BTA monomer on the surfaces of the C_{12}BTA or C_{13}BTA polymer. Hence, the surface of these polymers can be thought of as a medium with a certain degree of fluidity, where the diffusion is dependent on the dynamics of the surface. The relative difference in the rate of monomer incorporation is also in perfect agreement with the UV absorption measurements (that are sensitive to the formation of hydrogen bonds). Also, in the UV absorption measurements, the copolymers of C_{10}BTA and C_{12}BTA were found to equilibrate a factor of 16 faster as compared to copolymers formed from C_{10}BTA and C_{13}BTA (Figure 3). As expected, the coordination of the C_{10}BTA monomer is correlated to the number of hydrogen bonds it forms with the monomers of the host polymer (see Supporting Information Figure S11).

To further validate these results, we performed well-tempered metadynamics simulations to obtain the free energy profile of the stacking to hotspot transition (0−1 coordination).[41,42] The blue line in Figure 6 shows that a C_{10}BTA monomer has to cross an energy barrier of ∼0.8 kcal/mol to diffuse along the surface of a C_{13}BTA polymer and subsequently reach an accessible hotspot (energy minimum at stacking distance from the hotspot r/r_0 = 1). The barrier is much smaller for the pathway of the C_{10}BTA monomer that is diffusing along the surface of the C_{12}BTA polymer (Figure 6, black line), which implies that the diffusion of a C_{10}BTA monomer on the surface of the C_{12}BTA polymer is easier. This corroborates the evidence that the C_{13}BTA surface is a "slower" medium for C_{10}BTA diffusion, as compared to the surface of C_{12}BTA.

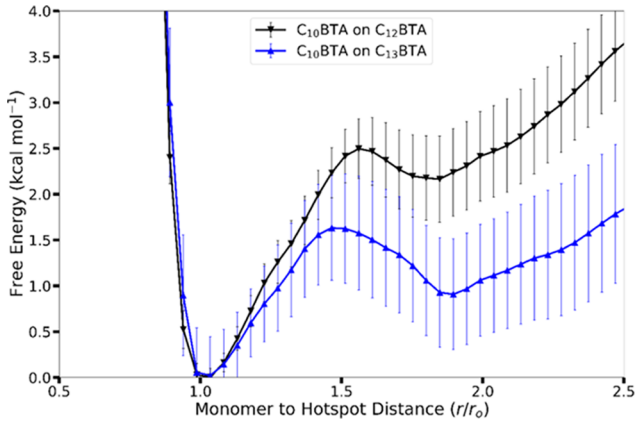

Figure 6. Free energy profile of a C_{10}BTA monomer along its pathway of incorporation into polymers formed from C_{12}BTA (black) and C_{13}BTA (blue). At r/r_0 = 1, C_{10}BTA is stacked onto a hotspot (i.e., incorporated in the host polymer). The error bars indicate the standard error of the mean calculated over four free energy profiles obtained from the metadynamics runs.

CONCLUSIONS

Supramolecular copolymers in water are a topic of recent interest, and the features that control the rates at which they form have yet to be addressed. In this contribution, we have reported the formation of supramolecular copolymers using a series of BTAs with differences in the length of the alkyl chains. Turbidity measurements indicated that supramolecular copolymers can be formed with new monomers being incorporated in a random fashion. To study the rates at which new monomers enter the different host polymers, we performed UV absorption measurements. These led us to conclude that the stability of the host polymer determines the rate at which new monomers can be incorporated in the polymers. We used a novel HDX-MS method that was inspired by the well-known pulse-labeling HDX technique to further support this conclusion. The experimental results are corroborated by CG-MD simulations. The C_{10}BTA monomers first adsorb and then diffuse on the polymer surface before becoming involved in hydrogen bonding. The diffusion phase takes longer on the surface of a host polymer that is less dynamic. In this approach, we have modeled the one-dimensional supramolecular polymers as visualized by Cryo-TEM as a single-molecule stack. Currently, we are performing detailed Cryo-TEM experiments for both copolymers and homopolymers, and in some cases, these studies point toward the existence of more complex nanostructures.

Future kinetic studies could systematically address the influence of other properties of the host polymers on the rates of copolymerization, for example, by involving aromatic, charge-transfer, or electrostatic interactions.[43−45] In addition, valuable information may be obtained by studying the susceptibility of polymers that are assembled using an isodesmic or cooperative polymerization mechanism to incorporate new monomers.[46] We anticipate that this kinetic experimental/computational approach will reveal more molecular structure to property relationships and thereby unlock the full potential of supramolecular polymers toward functional architectures and materials. Moreover, these insights into synthetic assemblies in water will be helpful to better understand the kinetics of the more complex natural multicomponent assemblies.

DOI: 10.1021/acs.macromol.9b00300
Macromolecules 2019, 52, 3049−3055

■ ASSOCIATED CONTENT

Supporting Information

The Supporting Information is available free of charge on the ACS Publications website at DOI: 10.1021/acs.macromol.9b00300.

Instrumentation and materials, experimental and computational procedures, infrared spectroscopy, CryoTEM, UV absorption spectroscopy, and HDX-MS. (PDF)

■ AUTHOR INFORMATION

Corresponding Author

*E-mail: e.w.meijer@tue.nl.

ORCID

René P. M. Lafleur: 0000-0003-0026-3428
Davide Bochicchio: 0000-0002-3682-9086
Björn Baumeier: 0000-0002-6077-0467
Anja R. A. Palmans: 0000-0002-7201-1548
Giovanni M. Pavan: 0000-0002-3473-8471
E. W. Meijer: 0000-0003-4126-7492

Notes

The authors declare no competing financial interest.

■ ACKNOWLEDGMENTS

We like to thank Dr Nicholas Matsumoto and Jolanda Spiering for providing samples of the molecules and Dr Simone Hendrikse for providing the artwork. The work was supported by the Dutch Ministry of Education, Culture and Science (Gravity program 024.001.035), the Innovational Research Incentives Scheme Vidi of the Netherlands Organisation for Scientific Research (NWO, project 723.016.002), and the Swiss National Science Foundation (SNSF, grant 200021_162827).

■ REFERENCES

(1) Dankers, P. Y. W.; Harmsen, M. C.; Brouwer, L. A.; Van Luyn, M. J. A.; Meijer, E. W. A modular and supramolecular approach to bioactive scaffolds for tissue engineering. *Nat. Mater.* **2005**, *4*, 568−574.

(2) Silva, G. A.; Czeisler, C.; Niece, K. L.; Beniash, E.; Harrington, D. A.; Kessler, J. A.; Stupp, S. I. Selective Differentiation of Neural Progenitor Cells by High-Epitope Density Nanofibers. *Science* **2004**, *303*, 1352−1355.

(3) Dankers, P. Y. W.; Boomker, J. M.; Huizinga-van der Vlag, A.; Wisse, E.; Appel, W. P. J.; Smedts, F. M. M.; Harmsen, M. C.; Bosman, A. W.; Meijer, W.; van Luyn, M. J. A. Bioengineering of living renal membranes consisting of hierarchical, bioactive supramolecular meshes and human tubular cells. *Biomaterials* **2011**, *32*, 723−733.

(4) Müller, M. K.; Brunsveld, L. A Supramolecular Polymer as a Self-Assembling Polyvalent Scaffold. *Angew. Chem., Int. Ed.* **2009**, *48*, 2921−2924.

(5) Straßburger, D.; Stergiou, N.; Urschbach, M.; Yurugi, H.; Spitzer, D.; Schollmeyer, D.; Schmitt, E.; Besenius, P. Mannose-Decorated Multicomponent Supramolecular Polymers Trigger Effective Uptake into Antigen-Presenting Cells. *ChemBioChem* **2018**, *19*, 912−916.

(6) Bakker, M. H.; Lee, C. C.; Meijer, E. W.; Dankers, P. Y. W.; Albertazzi, L. Multicomponent Supramolecular Polymers as a Modular Platform for Intracellular Delivery. *ACS Nano* **2016**, *10*, 1845−1852.

(7) Kim, I.; Han, E. H.; Ryu, J.; Min, J.-Y.; Ahn, H.; Chung, Y.-H.; Lee, E. One-Dimensional Supramolecular Nanoplatforms for Theranostics Based on Co-Assembly of Peptide Amphiphiles. *Biomacromolecules* **2016**, *17*, 3234−3243.

(8) Besenius, P.; Heynens, J. L. M.; Straathof, R.; Nieuwenhuizen, M. M. L.; Bomans, P. H. H.; Terreno, E.; Aime, S.; Strijkers, G. J.; Nicolay, K.; Meijer, E. W. Paramagnetic self-assembled nanoparticles as supramolecular MRI contrast agents. *Contrast Media Mol. Imaging* **2012**, *7*, 356−361.

(9) Bull, S. R.; Guler, M. O.; Bras, R. E.; Venkatasubramanian, P. N.; Stupp, S. I.; Meade, T. J. Magnetic Resonance Imaging of Self-Assembled Biomaterial Scaffolds. *Bioconjugate Chem.* **2005**, *16*, 1343−1348.

(10) Ortony, J. H.; Newcomb, C. J.; Matson, J. B.; Palmer, L. C.; Doan, P. E.; Hoffman, B. M.; Stupp, S. I. Internal dynamics of a supramolecular nanofibre. *Nat. Mater.* **2014**, *13*, 812−816.

(11) Albertazzi, L.; van der Zwaag, D.; Leenders, C. M. A.; Fitzner, R.; van der Hofstad, R. W.; Meijer, E. W. Probing Exchange Pathways in One-Dimensional Aggregates with Super-Resolution Microscopy. *Science* **2014**, *344*, 491−495.

(12) Hendrikse, S. I. S.; Wijnands, S. P. W.; Lafleur, R. P. M.; Pouderoijen, M. J.; Janssen, H. M.; Dankers, P. Y. W.; Meijer, E. W. Controlling and tuning the dynamic nature of supramolecular polymers in aqueous solutions. *Chem. Commun.* **2017**, *53*, 2279−2282.

(13) Pujals, S.; Tao, K.; Terradellas, A.; Gazit, E.; Albertazzi, L. Studying structure and dynamics of self-assembled peptide nanostructures using fluorescence and super resolution microscopy. *Chem. Commun.* **2017**, *53*, 7294−7297.

(14) Görl, D.; Soberats, B.; Herbst, S.; Stepanenko, V.; Wurthner, F. Perylene bisimide hydrogels and lyotropic liquid crystals with temperature-responsive color change. *Chem. Sci.* **2016**, *7*, 6786−6790.

(15) Rao, K. V.; George, S. J. Supramolecular Alternate Co-Assembly through a Non-Covalent Amphiphilic Design: Conducting Nanotubes with a Mixed D−A Structure. *Chem. - Eur. J.* **2012**, *18*, 14286−14291.

(16) Fernandez-Castano Romera, M.; Lafleur, R. P. M.; Guibert, C.; Voets, I. K.; Storm, C.; Sijbesma, R. P. Strain Stiffening Hydrogels through Self-Assembly and Covalent Fixation of Semi-Flexible Fibers. *Angew. Chem., Int. Ed.* **2017**, *56*, 8771−8775.

(17) Kieltyka, R. E.; Pape, A. C. H.; Albertazzi, L.; Nakano, Y.; Bastings, M. M. C.; Voets, I. K.; Dankers, P. Y. W.; Meijer, E. W. Mesoscale Modulation of Supramolecular Ureidopyrimidinone-Based Poly(ethylene glycol) Transient Networks in Water. *J. Am. Chem. Soc.* **2013**, *135*, 11159−11164.

(18) Besenius, P. Controlling supramolecular polymerization through multicomponent self-assembly. *J. Polym. Sci., Part A: Polym. Chem.* **2017**, *55*, 34−78.

(19) Fukui, T.; Kawai, S.; Fujinuma, S.; Matsushita, Y.; Yasuda, T.; Sakurai, T.; Seki, S.; Takeuchi, M.; Sugiyasu, K. Control over differentiation of a metastable supramolecular assembly in one and two dimensions. *Nat. Chem.* **2017**, *9*, 493−499.

(20) Ogi, S.; Stepanenko, V.; Thein, J.; Würthner, F. Impact of Alkyl Spacer Length on Aggregation Pathways in Kinetically Controlled Supramolecular Polymerization. *J. Am. Chem. Soc.* **2016**, *138*, 670−678.

(21) Greciano, E. E.; Matarranz, B.; Sanchez, L. Pathway Complexity Versus Hierarchical Self-Assembly in N-Annulated Perylenes: Structural Effects in Seeded Supramolecular Polymerization. *Angew. Chem., Int. Ed.* **2018**, *57*, 4697−4701.

(22) Cui, H.; Cheetham, A. G.; Pashuck, E. T.; Stupp, S. I. Amino Acid Sequence in Constitutionally Isomeric Tetrapeptide Amphiphiles Dictates Architecture of One-Dimensional Nanostructures. *J. Am. Chem. Soc.* **2014**, *136*, 12461−12468.

(23) Pramanik, P.; Ray, D.; Aswal, V. K.; Ghosh, S. Supramolecularly Engineered Amphiphilic Macromolecules: Molecular Interaction Overrules Packing Parameters. *Angew. Chem., Int. Ed.* **2017**, *56*, 3516−3520.

(24) Yu, Z.; Erbas, A.; Tantakitti, F.; Palmer, L. C.; Jackman, J. A.; Olvera de la Cruz, M.; Cho, N.-J.; Stupp, S. I. Co-assembly of Peptide

DOI: 10.1021/acs.macromol.9b00300
Macromolecules 2019, 52, 3049−3055

Amphiphiles and Lipids into Supramolecular Nanostructures Driven by Anion−π Interactions. *J. Am. Chem. Soc.* **2017**, *139*, 7823−7830.
(25) Görl, D.; Zhang, X.; Stepanenko, V.; Würthner, F. Supramolecular block copolymers by kinetically controlled co-self-assembly of planar and core-twisted perylene bisimides. *Nat. Commun.* **2015**, *6*, 7009.
(26) Pal, A.; Malakoutikhah, M.; Leonetti, G.; Tezcan, M.; Colomb-Delsuc, M.; Nguyen, V. D.; van der Gucht, J.; Otto, S. Controlling the Structure and Length of Self-Synthesizing Supramolecular Polymers through Nucleated Growth and Disassembly. *Angew. Chem., Int. Ed.* **2015**, *54*, 7852−7856.
(27) Ardoña, H. A. M.; Draper, E. R.; Citossi, F.; Wallace, M.; Serpell, L. C.; Adams, D. J.; Tovar, J. D. Kinetically Controlled Coassembly of Multichromophoric Peptide Hydrogelators and the Impacts on Energy Transport. *J. Am. Chem. Soc.* **2017**, *139*, 8685−8692.
(28) Ahlers, P.; Fischer, K.; Spitzer, D.; Besenius, P. Dynamic Light Scattering Investigation of the Kinetics and Fidelity of Supramolecular Copolymerizations in Water. *Macromolecules* **2017**, *50*, 7712−7720.
(29) Frisch, H.; Unsleber, J. P.; Lüdeker, D.; Peterlechner, M.; Brunklaus, G.; Waller, M.; Besenius, P. pH-Switchable Ampholytic Supramolecular Copolymers. *Angew. Chem., Int. Ed.* **2013**, *52*, 10097−10101.
(30) Markvoort, A. J.; Eikelder, H. M. M. t; Hilbers, P. A. J.; de Greef, T. F. A. Fragmentation and Coagulation in Supramolecular (Co)polymerization Kinetics. *ACS Cent. Sci.* **2016**, *2*, 232−241.
(31) Bochicchio, D.; Pavan, G. M. From Cooperative Self-Assembly to Water-Soluble Supramolecular Polymers Using Coarse-Grained Simulations. *ACS Nano* **2017**, *11*, 1000−1011.
(32) Bochicchio, D.; Salvalaglio, M.; Pavan, G. M. Into the Dynamics of a Supramolecular Polymer at Submolecular Resolution. *Nat. Commun.* **2017**, *8*, 147.
(33) Torchi, A.; Bochicchio, D.; Pavan, G. M. How the Dynamics of a Supramolecular Polymer Determines Its Dynamic Adaptivity and Stimuli-Responsiveness: Structure−Dynamics−Property Relationships From Coarse-Grained Simulations. *J. Phys. Chem. B* **2018**, *122*, 4169−4178.
(34) Thota, B. N. S.; Lou, X.; Bochicchio, D.; Paffen, T. F. E.; Lafleur, R. P. M.; van Dongen, J. L. J.; Ehrmann, S.; Haag, R.; Pavan, G. M.; Palmans, A. R. A.; Meijer, E. W. Supramolecular Copolymerization as a Strategy to Control the Stability of Self-Assembled Nanofibers. *Angew. Chem., Int. Ed.* **2018**, *57*, 6843−6847.
(35) Leenders, C. M. A.; Baker, M. B.; Pijpers, I. A. B.; Lafleur, R. P. M.; Albertazzi, L.; Palmans, A. R. A.; Meijer, E. W. Supramolecular polymerisation in water; elucidating the role of hydrophobic and hydrogen-bond interactions. *Soft Matter* **2016**, *12*, 2887−2893.
(36) Lou, X.; Lafleur, R. P. M.; Leenders, C. M. A.; Schoenmakers, S. M. C.; Matsumoto, N. M.; Baker, M. B.; van Dongen, J. L. J.; Palmans, A. R. A.; Meijer, E. W. Dynamic diversity of synthetic supramolecular polymers in water as revealed by hydrogen/deuterium exchange. *Nat. Commun.* **2017**, *8*, 15420.
(37) Zhang, Q.; Weber, C.; Schubert, U. S.; Hoogenboom, R. Thermoresponsive polymers with lower critical solution temperature: from fundamental aspects and measuring techniques to recommended turbidimetry conditions. *Mater. Horiz.* **2017**, *4*, 109−116.
(38) Fuller, J. M.; Raghupathi, K. R.; Ramireddy, R. R.; Subrahmanyam, A. V.; Yesilyurt, V.; Thayumanavan, S. Temperature-Sensitive Transitions below LCST in Amphiphilic Dendritic Assemblies: Host−Guest Implications. *J. Am. Chem. Soc.* **2013**, *135*, 8947−8954.
(39) Raghupathi, K. R.; Sridhar, U.; Byrne, K.; Raghupathi, K.; Thayumanavan, S. Influence of Backbone Conformational Rigidity in Temperature-Sensitive Amphiphilic Supramolecular Assemblies. *J. Am. Chem. Soc.* **2015**, *137*, 5308−5311.
(40) Konermann, L.; Simmons, D. A. Protein-folding kinetics and mechanisms studied by pulse-labeling and mass spectrometry. *Mass Spectrom. Rev.* **2003**, *22*, 1−26.
(41) Barducci, A.; Bussi, G.; Parrinello, M. Well-Tempered Metadynamics: A Smoothly Converging and Tunable Free-Energy Method. *Phys. Rev. Lett.* **2008**, *100*, 020603.
(42) Laio, A.; Parrinello, M. Escaping free-energy minima. *Proc. Natl. Acad. Sci. U.S.A.* **2002**, *99*, 12562−12566.
(43) Gabriel, G. J.; Iverson, B. L. Aromatic Oligomers that Form Hetero Duplexes in Aqueous Solution. *J. Am. Chem. Soc.* **2002**, *124*, 15174−15175.
(44) Rao, K. V.; Jayaramulu, K.; Maji, T. K.; George, S. J. Supramolecular Hydrogels and High-Aspect-Ratio Nanofibers through Charge-Transfer-Induced Alternate Coassembly. *Angew. Chem., Int. Ed.* **2010**, *49*, 4218−4222.
(45) Frisch, H.; Nie, Y.; Raunser, S.; Besenius, P. pH-Regulated Selectivity in Supramolecular Polymerizations: Switching between Co- and Homopolymers. *Chem. - Eur. J.* **2015**, *21*, 3304−3309.
(46) Casellas, N. M.; Pujals, S.; Bochicchio, D.; Pavan, G. M.; Torres, T.; Albertazzi, L.; Garcia-Iglesias, M. From Isodesmic to Highly Cooperative: Reverting Supramolecular Polymerization Mechanism in Water by Fine Monomer Design. *Chem. Commun.* **2018**, *54*, 4112−4115.

DOI: 10.1021/acs.macromol.9b00300
Macromolecules 2019, 52, 3049−3055